

Imaging of bioluminescent *Klebsiella pneumoniae* induced pulmonary infection in an immunosuppressed mouse model

Xing Hu¹, Yun Cai^{1,2,#} , Yuhang Wang¹,
Rui Wang², Jin Wang² and Bo Zhang^{1,3,#}

Abstract

Objective: To establish a mouse model of bioluminescent *Klebsiella pneumoniae*-induced lung infection, under different infection states after pretreatment with various dosages of cyclophosphamide (CTX).

Methods: A *K. pneumoniae* strain carrying the *luxCDABE* operon was used to infect immunocompetent mice (intraperitoneal injection of saline at 4 days and 1 day prior to experimental lung infection) and immunodeficient mice (50 mg/kg CTX at 4 days and 50 mg/kg CTX at 1 day prior to lung infection; or 150 mg/kg CTX at 4 days and 100 mg/kg CTX at 1 day prior to lung infection). Disease progression was monitored in living mice using a bioluminescence imaging system. The bioluminescent images, bacterial loads in lungs, blood cytological changes and histopathology of lungs were analysed.

Results: *K. pneumoniae*-induced lung infection models were established in mice pretreated with CTX. Different doses of CTX led to different severities of lung infection. Mice pretreated with 150/100 mg/kg CTX were more suitable for real-time monitoring as they had more typical bioluminescent images of lung infection, more obvious changes in the bioluminescent intensity values, more bacterial colonies in the lungs and more distinct pulmonary pathological changes.

Conclusions: A stable bioluminescent *K. pneumoniae*-induced lung infection model was successfully established in mice pretreated with CTX, which can be semi-quantitatively monitored in real-time.

#These authors contributed equally to this work.

Corresponding author:

Bo Zhang, Department of Respiratory Medicine, Air Force General Hospital, PLA, 30 Fu Cheng Road, 100142, Beijing, China.

Email: zhangbohuxi@sina.com

¹Medical School of Chinese PLA, Beijing, China

²Department of Pharmacy, Centre of Medicine Clinical Research, PLA General Hospital, Beijing, China

³Department of Respiratory Medicine, Air Force General Hospital, PLA, Beijing, China



Keywords

Klebsiella pneumoniae, bioluminescence, pneumonia, mouse model, cyclophosphamide

Date received: 25 February 2020; accepted: 4 August 2020

Introduction

Klebsiella pneumoniae is a common fermentative Gram-negative pathogen that can cause health-associated infections.¹ It usually resides in soil, surface water and on medical instruments.² *K. pneumoniae* strains have gained increasingly high levels of antimicrobial resistance; 61.4% of the strains are multidrug-resistant, 22% are extensively drug-resistant and 1.8% are pan-drug-resistant.³ *K. pneumoniae* has a natural resistance to ampicillin;⁴ and an individual point mutation of the *blaSHV-1* gene can help these bacteria hydrolyse the majority of penicillin and extended-spectrum cephalosporins, including cefuroxime, aztreonam and third- or fourth-generation cephalosporins.³ Moreover, the number of *K. pneumoniae* strains producing newer β -lactamases (carbapenem-hydrolysing enzymes) is increasing.^{5,6} The carbapenemase-producing *K. pneumoniae* has become an important nosocomial pathogen causing severe infections in critically-ill patients.⁷

Cyclophosphamide (CTX) is a classical myelotoxic agent, which is extensively applied as an immunosuppressive and anti-neoplastic agent in clinical practice. It is used in animal experiments to establish immunosuppressive models.⁸ As a conditioned pathogen, *K. pneumoniae* strains have weak virulence in healthy mice.⁹ Therefore, it is necessary to induce immunosuppression in mice before lung infection. Different CTX doses lead to different immune and lung infection status in mice.¹⁰

Bioluminescence is caused by a luciferase-catalysed reaction. *LuxCDABE*, the bacterial luciferase cassette, can produce bioluminescence at a wavelength of 490 nm by synthesizing all the required substrate compounds.¹¹ Real-time tracking of *K. pneumoniae* strains with *luxCDABE* operons in mouse tissues can be achieved using a bioluminescence imaging (BLI) system. However, no real-time monitoring of the *K. pneumoniae*-induced mouse lung infection model has been reported previously.

The present study aimed to establish a quantifiable and stable mouse model of bioluminescent *K. pneumoniae*-induced lung infection and to explore different infection states after pretreatment with various dosages of CTX to select the appropriate CTX dose for model establishment.

Materials and methods

Bacterial strains and preparation of inoculate

The bioluminescent strain *K. pneumoniae* Xen 39 (PerkinElmer, Waltham, MA, USA) was constructed by introduction of a copy of the *luxCDABE* operon on the chromosome through conjugation and transposition of a special plasmid. *K. pneumoniae* was cultured in Muller–Hinton agar (Becton, Dickinson and Company, Franklin Lakes, NJ, USA). The freshly plated *K. pneumoniae* was cultured in Mueller–Hinton broth to logarithmic phase at 37°C for 6 h. Finally,

K. pneumoniae was suspended at 1.0 McFarland by Densimat photometer (BioMérieux, Marcy l'Etoile, France).

Animals

Specific-pathogen-free, male ICR mice aged 8–10 weeks old weighing 30–35 g were used for all of the experiments (Medical Experimental Animal Centre, PLA General Hospital, Beijing, China). Using a 12-h light/12-h dark cycle, animals were housed in quiet individual cages at room temperature (20–26 °C) and humidity (50–70%) with free access to mouse chow and sterile water for 1 week before the experiments were undertaken. The mice were maintained according to the National Standards for Laboratory Animals of China (GB 14925-2010). All studies were approved by the Institutional Animal Care and Use Committee of the PLA General Hospital on 6 January 2019 (no. 2019-X15-71). The ARRIVE guidelines were followed for all animal experiments.¹²

Immunosuppressed murine lung infection models

An aqueous solution of CTX (Lot. MKCG546; Sigma-Aldrich, St Louis, MO, USA) was freshly prepared prior to the experiments and sterilized by passing through a 0.2- μ m syringe filter. A total of 36 mice were randomly and evenly divided into six groups (groups 1–6), including two control groups (groups 1 and 4) and four immunosuppressed groups (groups 2, 3, 5 and 6). In the control groups, mice were intraperitoneally injected with saline solution. Mice in group 1 were sacrificed by cervical dislocation at 24 h post-infection, while mice in group 4 were sacrificed at 48 h post-infection. For the four immunosuppressed groups, two groups of mice (groups 2 and 5) were injected with 50 mg/kg CTX at 4 days and 50 mg/kg CTX at 1 day prior

to lung infection (the CTX dose is shown as 50/50 mg/kg). Mice in group 2 were sacrificed at 24 h post-infection, while mice in group 5 were sacrificed at 48 h post-infection. In the other two immunosuppressed groups (groups 3 and 6), mice were injected with 150 mg/kg CTX at 4 days and 100 mg/kg at 1 day prior to lung infection (the CTX dose is shown as 150/100 mg/kg).^{13–15} Mice in group 3 were sacrificed at 24 h post-infection, while mice in group 6 were sacrificed at 48 h post-infection. After being intraperitoneally anaesthetized using 1% pentobarbital sodium solution (50 mg/kg; XiangBo Biotechnology, Guangdong, China), the mice were placed on an angle-adjustable work stand suspended by their incisors. The alternating glottis opening and closing could be observed using the oto speculum illuminating the oral cavity of the mouse. Subsequently, a one-time orotracheal intubation catheter (PN 000A3747 Mouse Intubation Pack; Hallowell EMC, Pittsfield, MS, USA) was inserted into the trachea through the glottis. Next, 100 μ l *K. pneumoniae* suspension at 1.0 McFarland (3×10^8 colony forming units [CFU]/ml) was slowly injected into the mouse trachea and the mouse was held vertically on the work stand for 1 min.

General status observations of mice

The general status of all mice was observed throughout the course of the study. The number of live and dead mice was recorded at 0, 6, 12, 24 and 48 h. Status of activity and mental state, such as reluctance to be active, fur piloerection, lackluster pelage, food intake reduction, water intake reduction and lethargy, were observed and recorded at each time-point described above.

In vivo BLI

The process of lung infection was monitored at 0, 6, 12, 24 and 48 h after inoculation. Briefly, mice in each group were lightly anaesthetized with sevoflurane and then placed into the camera obscura of a NightOWL II LB 983 *in vivo* imaging system (Berthold Technologies, Bad Wildbad, Germany). The exposure time was 30 sec. The amount of electric photons emitted from regions of interest per second (counts per second [cps]), which were released by the bioluminescent *K. pneumonia*, was quantitatively analysed by IndiGO 2.0.3.1 (Berthold Technologies, Bad Wildbad, Germany). The polychromatic bar shows the signal intensity, in which red represents high bioluminescent signals and blue represents low bioluminescent signals.

Cytological analysis in peripheral blood

Blood samples were collected from the caudal vein at 24 h or 48 h after lung infection. These samples were tested using a BC-2800 Vet small animal automatic haematology analyser (Mindray Biomedical Electronic Company, Guangdong, China). The white blood cell (WBC) and lymphocyte counts were quantified.

Bacterial enumeration

The mice were sacrificed by cervical dislocation after blood samples were harvested. The right lung lobes of each mouse were dissected and homogenized in 2 ml of 20 mM phosphate-buffered saline (pH 7.4) on ice for 5 min. The tissue homogenates were serially diluted by 10-fold dilution and a 100- μ l aliquot was evenly spread on Mueller–Hinton agar plates. After incubation at 37°C for 18 h, the colonies on plates were counted and expressed as CFU/g of lung.

Morphology assessment

The left lung specimens were fixed in 10% paraformaldehyde for 72 h, embedded in paraffin and sectioned into 4- μ m-thick slices, followed by staining with haematoxylin and eosin. Images were acquired under an Olympus PM-10 AD optical microscope and photographic system (Olympus, Tokyo, Japan). Lung injury was scored according to four aspects: (i) alveolar septal congestion; (ii) haemorrhage; (iii) aggregation or infiltration of neutrophils into the alveolus; (iv) strands of fibrin in the alveolus. Each item was graded using a four-point scale: 3, maximal damage; 2, moderate damage; 1, mild damage; 0, minimal (little) damage. The score was calculated according to the formula as follows: injury score = ([alveolar haemorrhage points/number of fields] + [alveolar septal congestion/no. of fields])/total number of alveoli counted + 2 \times (alveolar infiltration points/number of fields) + 3 \times (fibrin points/number of fields).¹⁶

Statistical analyses

All statistical analyses were performed using GraphPad Prism software version 8.0 (GraphPad Software, San Diego, CA, USA). Groups were compared using one-way analysis of variance followed by Dunnett's test. A *P*-value < 0.05 was considered as statistically significant.

Results

During the observation period, no deaths occurred in any group. Negative indicators of their general health status, such as reluctance to be active, lethargy, fur piloerection, lackluster pelage, food intake reduction and water intake reduction, were observed in all mice. The immunosuppressed mice had more severe symptoms compared with the immunocompetent mice. Mice in groups 2, 3, 5 and 6 all had signs of lethargy, fur

piloerection, lackluster pelage, food intake reduction and water intake reduction before being sacrificed, while only two mice in group 1 had signs of fur piloerection and lackluster pelage, and only three mice in group 4 had signs of fur piloerection, lackluster pelage, food intake reduction and water intake reduction. Furthermore, the immunosuppressed mice with the larger dose of CTX and longer infection time exhibited worse physical conditions than the other groups. For example, all mice in group 6 at 48 h post-infection were reluctant to be active and refused to intake food and water, while no mice in group 1 at 24 h post-infection had these signs.

The bioluminescent signals of the *K. pneumoniae* strain reflected the infected regions of the mouse lungs. The signal

intensity changed along with the change in duration of infection. In order to compare these signals under identical conditions, a predefined setting of 50 to 20 000 cps was applied for all measurements. The mice were checked with the imaging system at 0, 6, 12, 24 and 48 h post-infection (Figure 1). The bioluminescent signals of immunocompetent mice in the control groups 1 and 4 all disappeared by 24 h post-infection, while the signals in the immunosuppressed mice in the other four groups were continuously increased over time. At the same time point, mice with 150/100 mg/kg CTX injections (groups 3 or 6) emitted more intense signals compared with the mice injected with 50/50 mg/kg CTX (groups 2 or 5) (Figure 2).

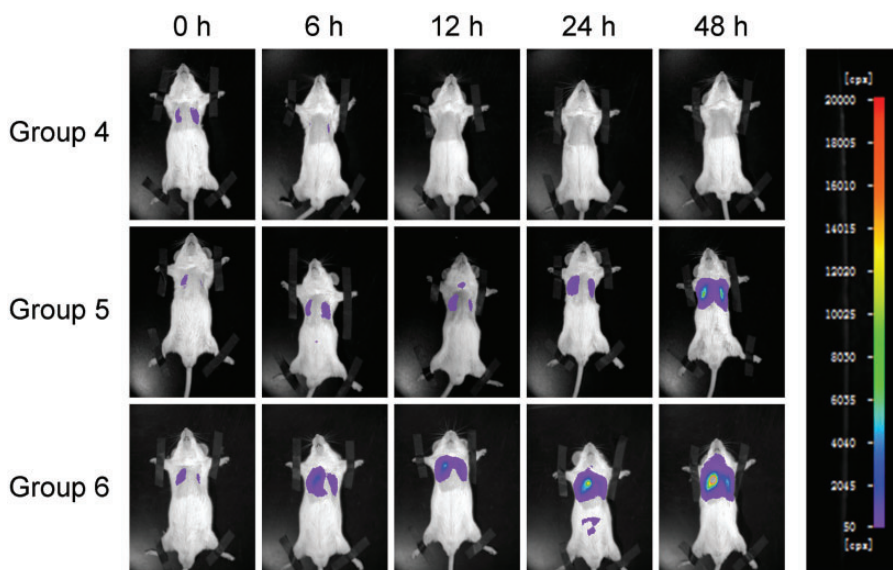


Figure 1. Representative bioluminescent monitoring images of *Klebsiella pneumoniae*-induced lung infection in mice ($n=6$ mice per group). A suspension of a bioluminescent *K. pneumoniae* strain (3×10^8 colony forming units/ml) was intratracheally inoculated into immunosuppressed mice. The polychromatic bar to the right of the images indicates the bioluminescent intensity and the counts per second (cps) value semi-quantitatively represents the bioluminescent intensity. Mice in group 4 were immunocompetent mice injected with saline prior to lung infection. Mice in group 5 were immunosuppressed mice injected with 50/50 mg/kg cyclophosphamide (CTX) prior to lung infection. Mice in group 6 were immunosuppressed mice injected with 150/100 mg/kg CTX prior to lung infection. Mice were monitored at 0 h, 6 h, 12 h, 24 h and 48 h after lung infection. The colour version of this figure is available at: <http://imr.sagepub.com>.

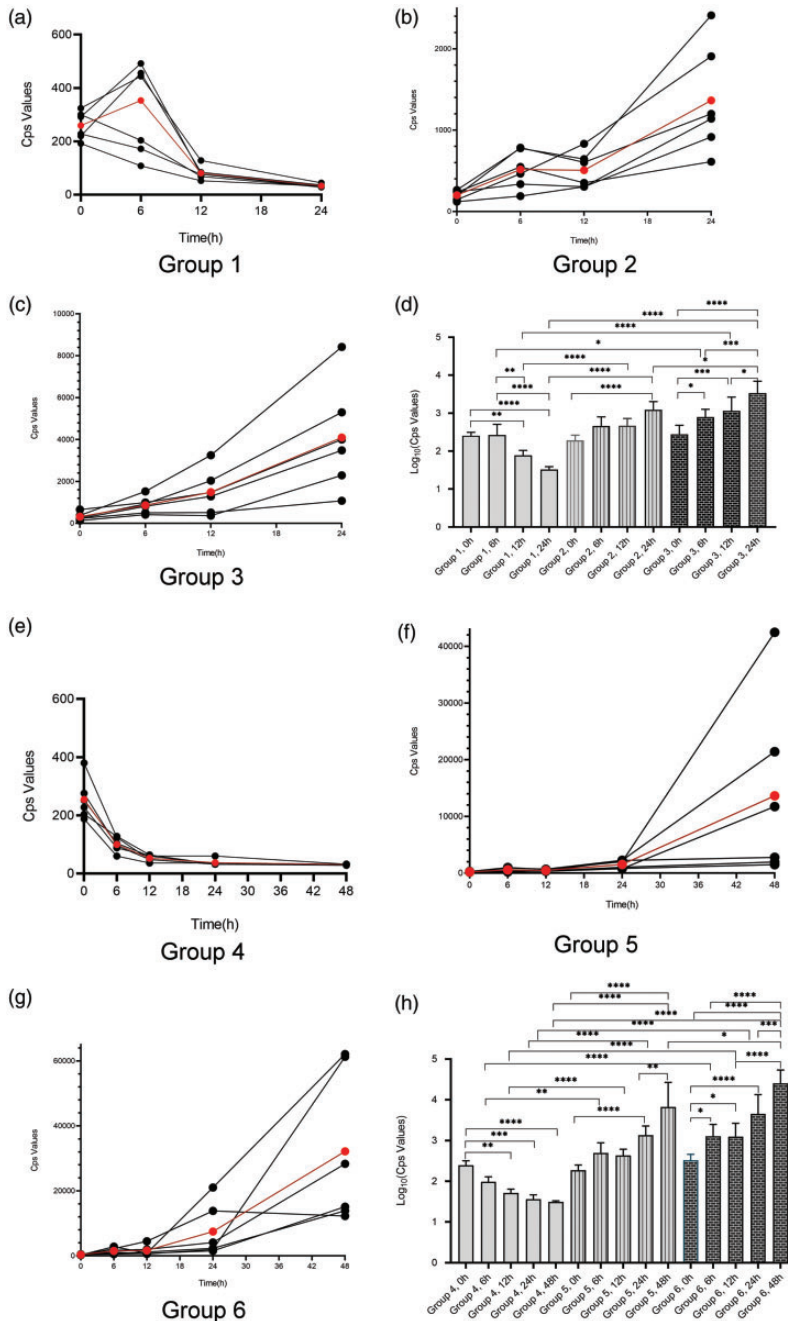


Figure 2. Changes in bioluminescent intensity as presented semi-quantitatively in counts per second (cps) in groups of mice with *Klebsiella pneumoniae*-induced lung infection ($n = 6$ mice per group). (a–c) Changes over 24 h in groups 1, 2 and 3. The red data points represent the mean cps for the six mice. (d) Statistical analyses of groups 1, 2 and 3. (e–g) Changes over 48 h in groups 4, 5 and 6. The red data points represent the mean cps for the six mice. (h) Statistical analyses of groups 4, 5 and 6. Data presented as mean \pm SD. * $P < 0.05$, ** $P < 0.01$, *** $P < 0.001$, **** $P < 0.0001$; one-way analysis of variance followed by Dunnett's test for group comparisons. The colour version of this figure is available at: <http://imr.sagepub.com>.

More detailed analyses of the changes in the bioluminescent signals of the *K. pneumoniae* strain in the lungs of mice are presented in Figure 2. In immunocompetent mice (control groups 1 and 4), the cps values peaked at 6 h post-infection or immediately after infection (Figures 2a and 2e). The cps values in these mice were decreased from 6 h to 12 h and all had declined to the lowest levels by 24 h post-infection (Figures 2a and 2e). Generally, the cps values of immunosuppressed mice injected with 50/50 mg/kg CTX (groups 2 and 5) slowly and steadily increased from 6 h to 12 h, then rapidly increased from 12 h to 24 h followed by an even more rapid increase from 24 h to 48 h (Figures 2b and 2f). The cps values of immunosuppressed mice injected with 150/100 mg/kg CTX (groups 3 and 6) exhibited similar changes compared with the mice in groups 2 and 5, but they demonstrated a higher growth rate (Figures 2c and 2g).

Details of the statistical analyses of the bioluminescent signals of the *K. pneumoniae* strain in the lungs of mice are presented in Figures 2d and 2h. At 0 h post-infection, there was no significant difference in bioluminescence signals between groups with different CTX dosages. Generally, at the same time point post-infection, mice in groups 2 and 3 had greater cps values compared with the control group 1; and mice in groups 5 and 6 had greater cps values compared with the control group 4; and there were statistical differences between these groups ($P < 0.05$). For example, at 24 h post-infection, group 3 mice showed significantly greater cps values compared with group 2 mice ($P < 0.001$); and at 48 h post-infection, group 6 mice showed much greater cps values compared with group 5 mice ($P < 0.05$). In addition, cps values of mice injected with the same CTX dosage were also significantly different at different time-points ($P < 0.05$).

All immunosuppressed mice showed significantly increased CFU values compared with the immunocompetent mice at the same time-point post-infection (Figure 3a) ($P < 0.001$ for all comparisons). Moreover, there were significant differences observed in mice with the same CTX dosage between 24 h and 48 h post-infection ($P < 0.001$ for both comparisons). However, there was no significant difference in CFU values between 50/50 mg/kg CTX group and 150/100 mg/kg CTX group at the same time-point post-infection. A strong positive correlation ($Y = 2.06 \times 10^{-6}X - 549$; $R^2 = 0.732$) was found between bacterial loads and cps values from the lungs of infected mice (Figure 3b).

Analysis of the WBC and lymphocyte counts in peripheral blood demonstrated that immunocompetent mice had significantly greater WBC and lymphocyte counts compared with the immunosuppressed mice at the same time-point post-infection ($P < 0.01$ for all comparisons). The immunocompetent mice at 48 h post-infection (group 4) had more WBCs but fewer lymphocytes compared with the mice at 24 h post-infection (group 1), but the differences did not reach statistical significance. The immunosuppressed mice with 50/50 mg/kg CTX injections at 48 h post-infection (group 5) had more WBCs and lymphocytes compared with the mice with 50/50 mg/kg CTX injections at 24 h post-infection (group 2), but the differences did not reach statistical significance. The mice with 150/100 mg/kg CTX injections at 48 h post-infection (group 6) had fewer WBCs and lymphocytes compared with the mice with 150/100 mg/kg CTX injections at 24 h post-infection (group 3), but the differences did not reach statistical significance. Overall, the immunosuppressed mice with 150/100 mg/kg CTX injections (groups 3 and 6) had lower WBC and lymphocyte counts compared with the mice with 50/50 mg/kg CTX injections (groups

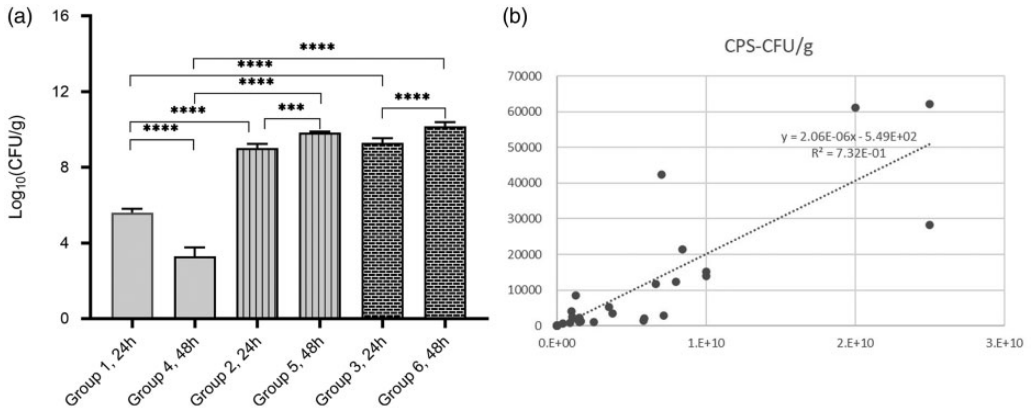


Figure 3. Bacterial loads in the right lungs post-infection ($n = 6$ mice per group). (a) Bacterial loads (colony forming units [CFU]/g) in the right lungs of infected mice. Data presented as mean \pm SD. **** $P < 0.001$, **** $P < 0.0001$; one-way analysis of variance followed by Dunnett's test for group comparisons. (b) The semi-quantitative counts per second (cps) values representing bioluminescent intensity and bacterial lung loads levels were closely related.

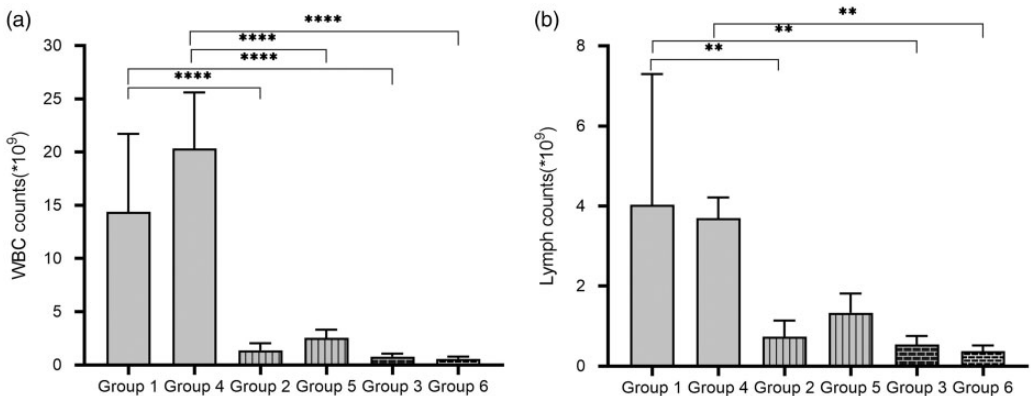


Figure 4. Blood cytological changes in mice ($n = 6$ mice per group). (a) White blood cell (WBC) count changes in mice. Results are presented as mean \pm SD. **** $P < 0.0001$; one-way analysis of variance followed by Dunnett's test for group comparisons. (b) Lymphocyte count changes in mice. Results are presented as mean \pm SD. ** $P < 0.01$; one-way analysis of variance followed by Dunnett's test for group comparisons. Statistical note: the lymphocyte counts for the six mice in group 1 showed a large inter-individual variation: $4.6 \times 10^9/l$, $10.1 \times 10^9/l$, $2.9 \times 10^9/l$, $3.8 \times 10^9/l$, $0.7 \times 10^9/l$ and $2.1 \times 10^9/l$. A normal-mode analysis of the data was undertaken and demonstrated normality. The dispersion was likely to have been influenced by the small sample size.

2 and 5), but the differences did not reach statistical significance.

All animals in the six groups had variable extents of lung injury, such as alveolar

haemorrhage, oedema, thickening of the alveolar septa and infiltration of neutrophilic cells into alveolar spaces and interstitial spaces. The most severe histological

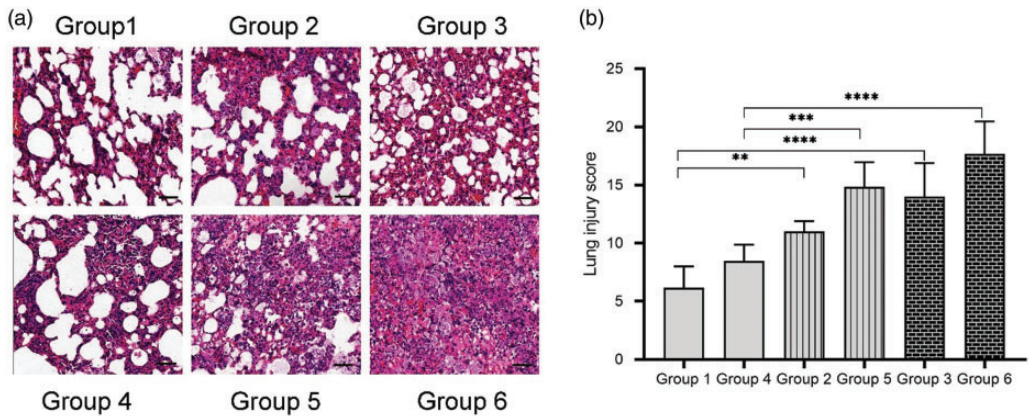


Figure 5. Representative histopathological images of the left lungs (haematoxylin and eosin stained) and lung injury scores of mice in the six groups ($n = 6$ mice per group). (a) Group 1, immunocompetent mouse, sacrificed at 24 h post-infection; group 2, immunocompetent mouse, sacrificed at 48 h post-infection; group 3, immunosuppressed mouse, injected 50/50 mg/kg cyclophosphamide (CTX), sacrificed at 24 h post-infection; group 4, immunosuppressed mouse, injected 50/50 mg/kg CTX, sacrificed at 48 h post-infection; group 5, immunosuppressed mouse, injected 150/100 mg/kg CTX, sacrificed at 24 h post-infection; group 6, immunosuppressed mouse, injected 150/100 mg/kg CTX, sacrificed at 48 h post-infection. Scar bar 50 μm . (b) Analysis of mouse lung injury scores in the six groups. The categories applied to generate the score were alveolar haemorrhage, alveolar septal congestion, intra-alveolar infiltrates and intra-alveolar fibrin deposition. Data presented as mean \pm SD. ** $P < 0.01$, *** $P < 0.001$, **** $P < 0.0001$; one-way analysis of variance followed by Dunnett's test for groups comparisons. The colour version of this figure is available at: <http://imr.sagepub.com>.

abnormalities could be found in the mice in group 6. Extensive airspaces were infiltrated with inflammatory cells, the alveolar septa were filled with apoptotic cells and haemorrhage areas could be easily found (Figure 5a, group 6). The mice in group 1 presented the least histopathological abnormalities (Figure 5a, group 1). The extent of these histological abnormalities was assessed by determining the lung injury scores (Figure 5b). At the same time-point post-infection, the lung injury scores of immunosuppressed mice were significantly higher compared with the immunocompetent mice ($P < 0.01$ for all comparisons). However, there was no significant difference observed between mice injected with the same CTX dose at 24 h and 48 h post-infection. In addition, no significant difference was found between the mice injected

with 50/50 mg/kg and 150/100 mg/kg CTX at the same time-point post-infection.

Discussion

Klebsiella pneumoniae can lead to a wide range of infections, including pneumonia, sepsis, bacteraemia, meningitis and pyogenic liver abscess for example. It causes serious infections in immunocompromised individuals in most cases, while the emergence of hypervirulent strains has increased the number of people susceptible to its infections.^{17,18} A suitable real-time monitoring animal model of pneumonia could be helpful for the study of *K. pneumoniae*-induced lung infection.

Due to its merits, such as non-toxicity, non-invasiveness, low cost, high throughput and easy administration, BLI has become

more generally applied by investigators for various studies.¹⁹ Bioluminescent bacteria, including *Mycobacterium tuberculosis*²⁰ and *Acinetobacter baumannii*,²¹ have been used in animal infection models for *in vivo* studies. However, no bioluminescent *K. pneumoniae* has been used in mouse models of lung infection. Bacterial luciferase is a dimer consisting of proteins encoded by the *lux A* and *lux B* genes, with the remainder of the *lux CDE* gene being responsible for the production of special proteins.¹¹ These proteins allow the luciferase to catalyse the production of light without the need of a substrate.²² *K. pneumoniae* carrying *lux CDABE* were clearly visible in the mouse lung in the current study. Moreover, the change of bioluminescence signal intensity reflected the infection status. The intensity of the bioluminescent signal was semi-quantitatively measured using cps values. The cps values were positively correlated with bacterial loads in the lungs (Figure 3b). Therefore, the cps values reflected the infection status of the mouse lungs. In addition, this lung infection mouse model could be used to visually and semi-quantitatively monitor the real-time process of lung infection, which would help reduce the number of experimental animals required.

A quantifiable and stable animal lung infection model is needed in order to prevent animal-to-animal variability. It is much harder to establish *in vivo* lung infection models compared with infections in other organs such as intra-abdominal organs, thigh, liver and skin, because the inoculated bacterial suspensions may obstruct the respiratory tract and cause the death of an animal. The amount of bacterial suspension injected into the mouse trachea, the methods used to inject the bacteria and the injection depth all play important roles in the successful construction of the model. In the present study, the mice were infected by intratracheally injecting

bacterial strains using a one-time orotracheal intubation catheter. Different from intranasal inoculation,²³ oral aspiration infection,²⁴ or infection after tracheotomy, intratracheal infection ensures that all bacteria were injected into the mouse lungs with little injury to the animals. This current study showed that there was no statistical difference between groups at 0 h post-infection, confirming the quantifiability of this mouse lung infection model (Figures 2d and 2h).

As an opportunistic pathogen, *K. pneumoniae* has weak virulence in healthy mice in the current study. BLI of infected immunocompetent mice showed that a large proportion of the bacteria were cleared out at 12 h post-infection (Figure 1, Figures 2a and 2e). In order to establish *K. pneumoniae* colonization, induction of immunodeficiency was needed prior to infection. Due to the impairment of the immune system, these mice would be more sensitive to pathogens. As a classical myelotoxic agent, CTX is used in many studies to establish immunocompromised animal models.^{8,13,25} Nonetheless, low doses or high doses of CTX cause mild or drastic immunosuppression, and suitable immunosuppression for pathogen inoculation should be further studied. In this current study, a regimen of intraperitoneal CTX injection at 4 days (150 mg/kg) and 1 day (100 mg/kg) before experimental infection was selected, as this protocol has been used to produce immunosuppressed models in approximately 5 days.^{10,26} The reduction of WBCs and lymphocytes were monitored by cytological analysis (Figures 4a and 4b). Moreover, the current study also explored 50/50 mg/kg CTX as a control dosage. Compared with immunocompetent mice, immunocompromised mice had fewer WBCs and lymphocytes in their blood. In addition, the WBC and lymphocyte counts were lower in mice injected with the higher doses of CTX compared with the lower doses. The

bacterial loads in immunosuppressed mice were significantly higher than those in healthy mice (Figure 3a) and the lung injuries in the immunosuppressed mice were much more severe than those in the immunocompetent mice (Figure 5). All of these results demonstrated that the immunocompromised state helped colonization and proliferation of *K. pneumoniae* in mouse lungs. Figures 1 and 2 show that mice with a higher dose of CTX exhibited stronger bioluminescence signals and faster increases in cps value compared with the mice treated with a lower dose at the same time-point or during the same time period. All of these findings suggest that the bacteria colonized more easily and proliferated more rapidly in the lungs of mice treated with 150/100 mg/kg CTX.

These current experimental results indicated that real-time monitoring of *K. pneumoniae*-induced lung infection could be achieved in immunosuppressed mice pretreated with CTX. Different doses of CTX led to different severities of lung infection. Lower doses of CTX led to milder lung infection. Future studies should determine the suitable CTX dose based on their research requirements. However, mice injected with 150/100 mg/kg CTX prior to lung infection were more suitable for real-time monitoring, because they had more typical bioluminescent images of lung infection, a more obvious increase in cps values, more bacterial colonies in the lungs and more distinct pulmonary pathological changes. In further research, based on the same level of immune system function, the bioluminescent mouse model could be used to evaluate the efficacy of antibiotic drugs with fewer experimental animals required.

In conclusion, the present study established a stable mouse model of bioluminescent *K. pneumoniae*-induced lung infection that can be semi-quantitatively monitored in real-time. The pretreatment with CTX at a dose of 150/100 mg/kg was appropriate

for the establishment of the model. Based on the same level of immune system function, the bioluminescent mouse model will be useful in evaluating the bactericidal effects of antibiotic drugs on *K. pneumoniae* with less experimental animals being required.


Declaration of conflicting interest

The authors declare that there are no conflicts of interest.

Funding

This study was supported by grants from the National Natural Science Foundation of China (no. 81770004) and the 13th Five-Year Plan of National Major Science and Technology Projects of China (no. 2018ZX09201-013).

ORCID iD

Yun Cai  <https://orcid.org/0000-0001-6687-9984>

References

1. Paczosa MK and Mecsas J. Klebsiella pneumoniae: Going on the Offense with a Strong Defense. *Microbiol Mol Biol Rev* 2016; 80: 629–661.
2. Rock C, Thom KA, Maxnick M, et al. Frequency of Klebsiella pneumoniae carbapenemase (KPC)-producing and non-KPC-producing Klebsiella species contamination of healthcare workers and the environment. *Infect control Hosp Epidemiol* 2014; 35: 426–429.
3. European Committee on Antimicrobial Susceptibility Testing. EUCAST guidelines for detection of resistance mechanisms and specific resistances of clinical and/or epidemiological importance, https://www.eucast.org/fileadmin/src/media/PDFs/EUCAST_files/Resistance_mechanisms/EUCAST_detection_of_resistance_mechanisms_170711.pdf (2017, accessed 10 September 2020).
4. Magiorakos AP, Srinivasan A, Carey RB, et al. Multidrug-resistant, extensively

- drug-resistant and pandrug-resistant bacteria: an international expert proposal for interim standard definitions for acquired resistance. *Clin Microbiol Infect* 2012; 18: 268–281.
5. da Silva RM, Traebert J and Galato D. Klebsiella pneumoniae carbapenemase (KPC)-producing Klebsiella pneumoniae: a review of epidemiological and clinical aspects. *Expert Opin Biol Ther* 2012; 12: 663–671.
 6. Li B, Yi Y, Wang Q, et al. Analysis of drug resistance determinants in Klebsiella pneumoniae isolates from a tertiary-care hospital in Beijing, China. *PLoS One* 2012; 7: e42280.
 7. Tofas P, Skiada A, Angelopoulou M, et al. Carbapenemase-producing Klebsiella pneumoniae bloodstream infections in neutropenic patients with haematological malignancies or aplastic anaemia: Analysis of 50 cases. *Int J Antimicrob Agents* 2016; 47: 335–339.
 8. Meng Y, Li B, Jin D, et al. Lactobacillus plantarum Immunomodulatory activity of KLDS1.0318 in cyclophosphamide-treated mice. *Food Nutr Res* 2018; 62: DOI: 10.29219/fnr.v62.1296.
 9. Wu JH and Tsai CG. Infectivity of hepatic strain Klebsiella pneumoniae in diabetic mice. *Exp Biol Med (Maywood)* 2005; 230: 757–761.
 10. Huyan XH, Lin YP, Gao T, et al. Immunosuppressive effect of cyclophosphamide on white blood cells and lymphocyte subpopulations from peripheral blood of Balb/c mice. *Int Immunopharmacol* 2011; 11: 1293–1297.
 11. Close D, Xu T, Smartt A, et al. The evolution of the bacterial luciferase gene cassette (lux) as a real-time bioreporter. *Sensors (Basel)* 2012; 12: 732–752.
 12. Kilkeny C, Browne W, Cuthill IC, et al. Animal research: reporting in vivo experiments: the ARRIVE guidelines. *Br J Pharmacol* 2010; 160: 1577–1579.
 13. Zhou YF, Tao MT, Huo W, et al. In Vivo Pharmacokinetic and Pharmacodynamic Profiles of Antofloxacin against Klebsiella pneumoniae in a Neutropenic Murine Lung Infection Model. *Antimicrob Agents Chemother* 2017; 61: e02691-16.
 14. Landersdorfer CB, Wang J, Wirth V, et al. Pharmacokinetics/pharmacodynamics of systemically administered polymyxin B against Klebsiella pneumoniae in mouse thigh and lung infection models. *J Antimicrob Chemother* 2018; 73: 462–468.
 15. Lepak AJ and Andes DR. In Vivo Pharmacodynamic Target Assessment of Delafloxacin against Staphylococcus aureus, Streptococcus pneumoniae, and Klebsiella pneumoniae in a Murine Lung Infection Model. *Antimicrob Agents Chemother* 2016; 60: 4764–4769.
 16. Matute-Bello G, Winn RK, Jonas M, et al. Fas (CD 95) induces alveolar epithelial cell apoptosis in vivo: implications for acute pulmonary inflammation. *Am J Pathol* 2001; 158: 153–161.
 17. Russo TA, Shon AS, Beanan JM, et al. Hypervirulent K. pneumoniae secretes more and more active iron-acquisition molecules than “classical” K. pneumoniae thereby enhancing its virulence. *PLoS One* 2011; 6: e26734.
 18. Magill SS, Edwards JR, Bamberg W, et al. Multistate point-prevalence survey of health care-associated infections. *N Engl J Med* 2014; 370: 1198–1208.
 19. Baker M. Whole-animal imaging: The whole picture. *Nature* 2010; 463: 977–980.
 20. Andreu N, Zelmer A, Sampson SL, et al. Rapid in vivo assessment of drug efficacy against Mycobacterium tuberculosis using an improved firefly luciferase. *J Antimicrob Chemother* 2013; 68: 2118–2127.
 21. Na SH, Oh MH, Jeon H, et al. Imaging of bioluminescent Acinetobacter baumannii in a mouse pneumonia model. *Microb Pathog* 2019; 137: 103784.
 22. Meighen EA. Molecular biology of bacterial bioluminescence. *Microbiol Rev* 1991; 55: 123–142.
 23. Michel LV, Kaur R, Zavorin M, et al. Intranasal coinfection model allows for assessment of protein vaccines against nontypeable Haemophilus influenzae in mice. *J Med Microbiol* 2018; 67: 1527–1532.
 24. Nielsen TB, Yan J, Luna B, et al. Murine Oropharyngeal Aspiration

- Model of Ventilator-associated and Hospital-acquired Bacterial Pneumonia. *J Vis Exp* 2018; 136: 57672.
25. Wicha WW, Strickmann DB and Paukner S. Pharmacokinetics/pharmacodynamics of lefamulin in a neutropenic murine pneumonia model with *Staphylococcus aureus* and *Streptococcus pneumoniae*. *J Antimicrob Chemother* 2019; 74(Suppl 3): iii11–iii18.
26. Craig WA, Redington J and Ebert SC. Pharmacodynamics of amikacin in vitro and in mouse thigh and lung infections. *J Antimicrob Chemother* 1991; 27(Suppl C): 29–40.